



Metabolic Reprogramming of Mouse Bone Marrow Derived Macrophages Following Erythrophagocytosis

Alexis Catala^{1,2}, Lyla A. Youssef³, Julie A. Reisz¹, Monika Dzieciatkowska¹, Nicholas E. Powers⁴, Carlo Marchetti⁴, Matthew Karafin⁵, James C. Zimring⁶, Krystalyn E. Hudson⁷, Kirk C. Hansen¹, Steven L. Spitalnik^{7*} and Angelo D'Alessandro^{1,8*}

¹ Department of Biochemistry and Molecular Genetics, University of Colorado Denver – Anschutz Medical Campus, Aurora, CO, United States, ² Program in Structural Biology and Biochemistry, University of Colorado Denver – Anschutz Medical Campus, Aurora, CO, United States, ³ Department of Microbiology and Immunology, Columbia University, New York, NY, United States, ⁴ Department of Medicine – Division of Infectious Diseases, University of Colorado Denver – Anschutz Medical Campus, Aurora, CO, United States, ⁵ Medical Sciences Institute, Blood Center of Wisconsin (Versiti), Milwaukee, WI, United States, ⁶ Department of Pathology, University of Virginia, Charlottesville, VA, United States, ⁷ Department of Pathology and Cell Biology, Columbia University, New York, NY, United States, ⁸ Department of Medicine – Division of Hematology, University of Colorado Denver – Anschutz Medical Campus, Aurora, CO, United States

OPEN ACCESS

Edited by:

Anna Bogdanova,
University of Zurich, Switzerland

Reviewed by:

Mauro Magnani,
University of Urbino Carlo Bo, Italy
Rosemary L. Sparrow,
Monash University, Australia

*Correspondence:

Steven L. Spitalnik
ss2479@cumc.columbia.edu
Angelo D'Alessandro
angelo.dalessandro@cuanschutz.edu

Specialty section:

This article was submitted to
Red Blood Cell Physiology,
a section of the journal
Frontiers in Physiology

Received: 26 February 2020

Accepted: 02 April 2020

Published: 30 April 2020

Citation:

Catala A, Youssef LA, Reisz JA, Dzieciatkowska M, Powers NE, Marchetti C, Karafin M, Zimring JC, Hudson KE, Hansen KC, Spitalnik SL and D'Alessandro A (2020) Metabolic Reprogramming of Mouse Bone Marrow Derived Macrophages Following Erythrophagocytosis. *Front. Physiol.* 11:396. doi: 10.3389/fphys.2020.00396

Reticuloendothelial macrophages engulf ~0.2 trillion senescent erythrocytes daily in a process called erythrophagocytosis (EP). This critical mechanism preserves systemic heme-iron homeostasis by regulating red blood cell (RBC) catabolism and iron recycling. Although extensive work has demonstrated the various effects on macrophage metabolic reprogramming by stimulation with proinflammatory cytokines, little is known about the impact of EP on the macrophage metabolome and proteome. Thus, we performed mass spectrometry-based metabolomics and proteomics analyses of mouse bone marrow-derived macrophages (BMDMs) before and after EP of IgG-coated RBCs. Further, metabolomics was performed on BMDMs incubated with free IgG to ensure that changes to macrophage metabolism were due to opsonized RBCs and not to free IgG binding. Uniformly labeled tracing experiments were conducted on BMDMs in the presence and absence of IgG-coated RBCs to assess the flux of glucose through the pentose phosphate pathway (PPP). In this study, we demonstrate that EP significantly alters amino acid and fatty acid metabolism, the Krebs cycle, OXPHOS, and arachidonate-linoleate metabolism. Increases in levels of amino acids, lipids and oxylipins, heme products, and RBC-derived proteins are noted in BMDMs following EP. Tracing experiments with U-¹³C₆ glucose indicated a slower flux through glycolysis and enhanced PPP activation. Notably, we show that it is fueled by glucose derived from the macrophages themselves or from the extracellular media prior to EP, but not from opsonized RBCs. The PPP-derived NADPH can then fuel the oxidative burst, leading to the generation of reactive oxygen species necessary to promote digestion of phagocytosed RBC proteins via radical attack. Results were confirmed by redox proteomics experiments, demonstrating the oxidation of Cys152 and Cys94 of glyceraldehyde 3-phosphate dehydrogenase (GAPDH) and hemoglobin-β, respectively. Significant increases in early Krebs cycle and C₅-branched dibasic acid metabolites

(α -ketoglutarate and 2-hydroxyglutarate, respectively) indicate that EP promotes the dysregulation of mitochondrial metabolism. Lastly, EP stimulated aminolevulinic acid (ALA) synthase and arginase activity as indicated by significant accumulations of ALA and ornithine after IgG-mediated RBC ingestion. Importantly, EP-mediated metabolic reprogramming of BMDMs does not occur following exposure to IgG alone. In conclusion, we show that EP reprograms macrophage metabolism and modifies macrophage polarization.

Keywords: macrophage metabolism, omics technologies, blood, OXPHOS, mitochondrial dysregulation, pentose phosphate pathway, lipid accumulation

INTRODUCTION

Erythrocyte (red blood cell, RBC) function extends beyond the monumental task of maintaining systemic acid/base equilibria via oxygen, carbon dioxide, and the transport of nutrients to tissues. Other vital roles include erythrocyte function [i.e., release of metabolically active molecules such as adenosine triphosphate (ATP) and nitric oxide (NO)], redox regulation, systemic hemodynamics, immunomodulation, and iron metabolism (Alayash et al., 2001; Kuhn et al., 2017). In adults, RBCs account for ~83% of the total cells in the body (25 out of ~30 trillion) and have an average lifespan of 120 days; thus, ~0.2 trillion RBCs are cleared from the bloodstream and generated *de novo* on a daily basis (Nemkov et al., 2018). Importantly, RBC damage and changes to deformability are directly linked to several severe pathologies (Casparly et al., 1967; Yoshida et al., 2019) including endothelial dysfunction (Kuhn et al., 2017), anemia (Alsultan et al., 2010; Belanger et al., 2015; Belcher et al., 2017), sepsis (Larsen et al., 2010), diabetic nephropathy (Brown et al., 2005), and thrombosis (Barr et al., 2013; Weisel and Litvinov, 2019).

Recycling of iron derived from RBCs is essential for sustaining erythropoiesis. As much as 70% of the total iron in the human body, or 3–5 g, is contained within RBCs, specifically in the heme protoporphyrin rings of hemoglobin (a single RBC contains ~1.0 billion heme moieties per ~250 million hemoglobin molecules; Gkouvatsos et al., 2012; Korolnek and Hamza, 2015; Yoshida et al., 2019). Notably, iron is a potent catalyst for generating reactive oxygen species (ROS) via the Fenton reaction, which can quickly lead to systemic toxicity due to the high reactivity of iron when free in the circulation (e.g., upon overload of transferrin, the plasma iron chaperone) (Papanikolaou and Pantopoulos, 2005; Kosman, 2010; Hod et al., 2010; Korolnek and Hamza, 2015; Rapido et al., 2017; Youssef and Spitalnik, 2017a). For this reason, highly specialized mechanisms are required for regulating RBC catabolism and iron recycling. To this end, macrophages are integral to the tight regulatory mechanism of RBC clearance (de Back et al., 2014; Klei et al., 2017) Reticuloendothelial macrophages (REMs), primarily in the spleen and liver, opsonize senescent RBCs in a process called erythrophagocytosis (EP) (Gkouvatsos et al., 2012; de Back et al., 2014).

With ~2 million RBCs being recycled every second via this mechanism, EP is the largest source of iron flux in the body (Korolnek and Hamza, 2015). Excessive EP by individual macrophages can lead to ferroptosis both *in vitro* and *in vivo*

(Dixon et al., 2012; Youssef and Spitalnik, 2017a). This form of iron-induced, non-apoptotic cell death is characterized by an overwhelming, iron-dependent accumulation of lethal ROS derived from lipid peroxidation (Dixon et al., 2012; Cao and Dixon, 2016). During this process, free radicals can strip electrons from unsaturated fatty acid components of membrane lipids, initiating a self-propagating chain reaction and massive oxidative destruction of lipids (Yang and Stockwell, 2016; Ramana et al., 2017). A bolus of intracellular iron and heme due to EP can also upregulate transcription of aminolevulinic acid (ALA) synthase, using glycine and succinyl-CoA from the Krebs cycle to produce ALA and initiate porphyrin (the heme precursor) synthesis. Other heme-responsive genes include heme oxygenase 1 (HO-1), a heme-catabolizing, and anti-inflammatory enzyme associated with maintaining the integrity of the REM lineage (Kovtunovych et al., 2010; Naito et al., 2014; Soares and Hamza, 2016), and SPI-C, a E26 transformation-specific (Ets) transcription factor required for the development of splenic and bone marrow (F4/80^{hi}) macrophages (Kohyama et al., 2009; Haldar et al., 2014). In the clinic, hypoferremia (iron-deficiency) and heme-catabolizing enzyme deficiencies (e.g., HO-1 deficiency) can cause progressive depletion of erythrophagocytic macrophage populations, profoundly deregulating heme-iron metabolism and homeostasis (Guida et al., 2015; Soares and Hamza, 2016).

Two major macrophage subsets (M1/M2) were identified, based on their polarization status, and defined by their different functional programs, migration mode, and cytokine secretion profiles (Labonte et al., 2014; Curi et al., 2017; Mould et al., 2017; Remmerie and Scott, 2018). Classically activated (M1) macrophages are described as proinflammatory macrophages that are more migratory in nature and release inflammatory cytokines, such as interleukin-6 (IL-6), interferon- γ (IFN- γ), and tumor necrosis factor- α (TNF- α), to aid in the amplification of immune responses and directed microenvironmental remodeling (Martinez and Gordon, 2014; Meiser et al., 2016; Gaber et al., 2017; Nonnenmacher and Hiller, 2018). By contrast, alternatively activated (M2) macrophages are typically less migratory owing to their extensive roles in repairing tissue-damage, and have a proresolution profile characterized by the secretion of cytokines, such as transforming growth factor- β (TGF- β), IL-4, IL-10, and IL-13 (Zhang and An, 2007; Nahrendorf and Swirski, 2013; Yang and Ming, 2014). Although the M1/M2 polarization nomenclature is helpful in binning macrophage subsets, macrophage populations are

actually quite heterogeneous, polarization is both transient and plastic, intermediate forms have been seen, and other subtypes have been proposed (e.g., M4, Mox, Mhem) (Sica and Mantovani, 2012; Nahrendorf and Swirski, 2013; Labonte et al., 2014; Youssef and Spitalnik, 2017b; Viola et al., 2019). The focus of the studies described herein will be on the metabolic differences between these subsets and not their cytokine profiles.

M1 macrophages exhibit a metabolic shift similar to the cancer-associated Warburg effect, in which the Krebs cycle has been altered and there are increases in lactate production and an amplified flux through the pentose phosphate pathway (PPP) (Kelly and O'Neill, 2015; Viola et al., 2019). Importantly, amplified PPP flux fuels the production of reduced nicotinamide adenine dinucleotide phosphate (NADPH), thereby promoting ROS generation via NADPH oxidase (Kelly and O'Neill, 2015). Increases in mitochondrial ROS can negatively affect Complex II activity in the electron transport chain, prompting accumulation of succinate (Zhao et al., 2019). Succinate can then stabilize hypoxia-inducible factor 1- α (HIF1 α) via inhibited hydroxylation, inducing expression of glycolytic enzymes and proinflammatory IL-1 β (Tannahill et al., 2013). M1 macrophages also have increased phenylalanine production, which promotes the expression and activity of GTP cyclohydrolase I (Li et al., 2007). This allows for directed modulation of tetrahydrobiopterin synthesis and, by extension, nitric oxide (NO) production (Li et al., 2007). In contrast, M2 macrophages are not as dependent on glycolysis for producing energy-fueling metabolites like ATP and, instead, rely more heavily on mitochondrial metabolism (Kelly and O'Neill, 2015; Noe and Mitchell, 2019; Viola et al., 2019). Their polarization state is partly mediated by increases in intracellular itaconate (an anti-inflammatory metabolite that activates Nrf2 via KEAP1 alkylation) (Mills et al., 2018; O'Neill and Artyomov, 2019) and arginine metabolism (Noe and Mitchell, 2019). Arginine is preferentially metabolized to produce ornithine and urea instead of NO via arginase 1 (Arg-1) to promote polyamine generation and HIF1 α destabilization (Kelly and O'Neill, 2015; Noe and Mitchell, 2019).

Fundamental to macrophage activity, metabolic reprogramming modulates key immune functions such as phagocytosis, inflammatory cytokine signaling, and extracellular matrix remodeling (Curi et al., 2017; Van den Bossche et al., 2017; Nonnenmacher and Hiller, 2018; D'Alessandro et al., 2018). Despite extensive evidence highlighting the central role of metabolic reprogramming following stimulation with proinflammatory factors (e.g., LPS, INF- γ) (Martinez and Gordon, 2014; Kelly and O'Neill, 2015), there is limited information that directly addresses the impact of phagocytosis itself on macrophage metabolism. To the best of our knowledge, no study has yet focused on these aspects within the framework of EP. Therefore, we addressed this deficit by conducting metabolomic analyses on bone marrow derived macrophages (BMDMs) that had phagocytosed IgG-opsonized RBCs. Given the metabolic derangement that can ensue due to heme-iron dysregulation, we hypothesize BMDMs that have engulfed iron-loaded RBCs will be burdened by increased oxidant stress and accumulate eicosanoids and oxylipins.

MATERIALS AND METHODS

Mice

Wild-type C57BL/6 mice (6–12 weeks of age) were purchased from Jackson Laboratories. All procedures were approved by the Institutional Animal Care and Use Committee at Columbia University (New York City, NY, United States). Each experiment was conducted at least twice in biological triplicates ($n = 3$ per group, each independent experiment).

RBC Collection

Mice were bled aseptically via cardiac puncture and pooled whole blood was placed in CPDA-1 solution obtained from human primary collection packs (Baxter International, Deerfield, IL, United States) to a final concentration of 15% CPDA-1. Whole blood was log4 leukofiltered using Neonatal High-efficiency Leukocyte Reduction Filters (Purecell Neo; Pall Corporation, Port Washington, NY, United States). RBCs from leukofiltered blood were packed by centrifugation (10 min, 4°C, 1,000 \times g) and a portion of the plasma-containing CPDA-1 supernatant was removed to yield a hematocrit of \sim 75%. Packed RBCs were used “fresh” (i.e., stored < 24 h at 4°C) to interrogate EP.

In vitro EP Assay

Mononuclear cells obtained from mouse femurs were cultured for 7–11 days in Iscove's Modified Dulbecco's Medium supplemented with 10% FBS, 2 mM L-glutamine, 50 units/ml penicillin, 50 μ g/mL streptomycin, 20 μ g/mL gentamycin (Thermo Fisher Scientific, Waltham, MA, United States) and 20 ng/mL human macrophage colony-stimulating factor (M-CSF) (PeproTech, Rocky Hill, NJ, United States) to generate primary BMDMs. Opsonized RBCs were generated by incubating RBCs with rabbit anti-mouse RBC IgG at 0.5 mg/mL (Rockland Immunochemicals, Limerick, PA, United States). Adherent BMDMs were plated 24 h prior to the experiment and incubated with PBS or opsonized RBCs for 2 h at 37°C. Following incubation, aliquots of the extracellular media were taken for metabolomic analysis of supernatants and non-ingested RBCs were lysed. Adherent BMDMs were washed with PBS, collected by scraping, and pelleted for metabolomic analysis of cell pellets.

In vitro IgG Assay

Mononuclear cells obtained from bone marrow of C57BL/6J mice were seeded at 1×10^6 cell/mL in a 48-well plate and differentiated for 7 days in RPMI 1,640 medium supplemented with 10% FCS, 1% penicillin/streptomycin (P/S) and 10 ng/mL M-CSF (R&D system; Minneapolis, MN, United States). Cells were then washed with (1x) PBS, and complete media in the absence of M-CSF was added to the cultures. Vehicle or mouse IgG (0.5 mg/mL) (R&D System, Minneapolis, MN, United States) were added for 1 h at 37°C. Following incubation, cells were washed and stored at -80°C for metabolomics. Thawed cells were lysed by adding lysis buffer directly to wells and removed by scraping.

Metabolic Labeling Experiments

Uniformly labeled $^{13}\text{C}_6$ -glucose (Cambridge Isotope Laboratories, Tewksbury, MA, United States) was incubated with RBCs (161 mM for 50% final ratio of labeled glucose) for 4 h at 37°C, before being gently washed with PBS to remove extracellular $^{13}\text{C}_6$ -glucose. For labeling BMDMs, $^{13}\text{C}_6$ -glucose was supplemented in the media used for culturing BMDMs (25 mM for 50% final ratio of labeled glucose) 1 h prior to, or during, EP. Samples were collected at 1, 3, and 12 h, and metabolites from cells extracted (in the absence of heavy labeled internal standards) for metabolomic analysis.

UHPLC-MS Metabolomics

Metabolites were extracted from cell pellets ($\sim 1 \times 10^6$ cells) or supernatants at a dilution of 1:10 or 1:25, respectively, in ice-cold lysis buffer (5:3:2 MeOH:ACN:H₂O) in the presence of a mix of heavy labeled internal standards. These standards included 15 uniformly labeled $^{13}\text{C}^{15}\text{N}$ -amino acids at a final concentration of 2.5 μM , $^{13}\text{C}_1$ -lactate (40 μM), $^{13}\text{C}_5$ -2- α -ketoglutarate, $^{13}\text{C}_4$ -succinate, $^{13}\text{C}_{1,4}$ -fumarate, 2H₄-prostaglandin E₂, and 2H₈-arachidonic acid at a final concentration of 1 μM (Cambridge Isotopes Laboratories, Inc., Tewksbury, MA, United States). Samples were vortexed, insoluble material pelleted, and supernatants collected. Extracts (20 μL) were injected into a Thermo Vanquish UHPLC system coupled to a Thermo Q Exactive mass spectrometer (Vanquish – Q Exactive; Thermo Fisher Scientific, San Jose, CA, United States and Bremen, Germany) with electrospray ionization for metabolomic analysis, as described (Catala et al., 2018). Technical mixes were generated by pooling aliquots of extracts and ran every 3 analytical runs to control for technical variability as judged by coefficients of variation (CVs). Metabolite assignments, isotopologue distributions, and correction for expected natural abundancies of ^{13}C were performed using MAVEN (Princeton, NJ, United States) (Melamud et al., 2010). Discovery mode analysis was performed with standard workflows using Compound Discoverer (Thermo Fisher Scientific, Waltham, MA, United States).

UHPLC-MS Lipidomics

Hydrophobic metabolites were extracted from cell pellets ($\sim 1 \times 10^6$ cells) in ice-cold methanol at a 1:10 dilution. Samples were quickly vortexed at room temperature followed by incubation at -20°C for 30 min and centrifugation (18,213 $\times g$, 10 min, 4°C). Supernatants (40 μL) were diluted 1:1 using 10 mM ammonium acetate and protein pellets stored at -80°C. Extracts (20 μL) were injected into our UHPLC-MS system with electrospray ionization. Metabolites were separated on a 150 \times 2.1 mm, 1.8 μm Acquity HSS T3 column (Waters, Milford, MA, United States) at 45°C using a 17 min gradient method at 300 $\mu\text{L}/\text{min}$ and mobile phases (A: 75:25 H₂O:ACN, 5 mM NH₄OAc; B: 50:45:5 IPA:ACN:H₂O, 5 mM NH₄OAc) for negative ion mode. Solvent gradient: 0–1.0 min 25% B; 1.0–2.0 min 50% B; 2.0–8.0 min 90% B; 8.0–10.0 min 99% B; 10.0–14.0 min hold at 99% B; 14.0–14.1 min 25% B, 400 $\mu\text{L}/\text{min}$; 14.1–16.9 min hold at 25% B, 400 $\mu\text{L}/\text{min}$; 16.9–17.0 min hold

at 25% B. Technical mixes were generated, ran and technical variability assessed, as described above.

Nano-UHPLC-Tandem MS Proteomics

Proteins extracted from BMDM cell pellets were separated by SDS-PAGE, and bands ranging from ~ 20 to 80 kDa were excised, reduced, alkylated, and trypsin digested. Extracted peptides were analyzed by nanoLCMS-MS (Thermo EASY-nLC 1,000 – Q Exactive HF; Thermo Fisher Scientific; San Jose, CA, United States and Bremen, Germany) and separated on a house-made 15 cm C18 analytical column (100 mm inner diameter) packed with Cortecs C18 resin (2.7 mm; Phenomenex, Torrance, CA, United States), using a 80 min linear gradient of 2–32% ACN at 350 nL/min.

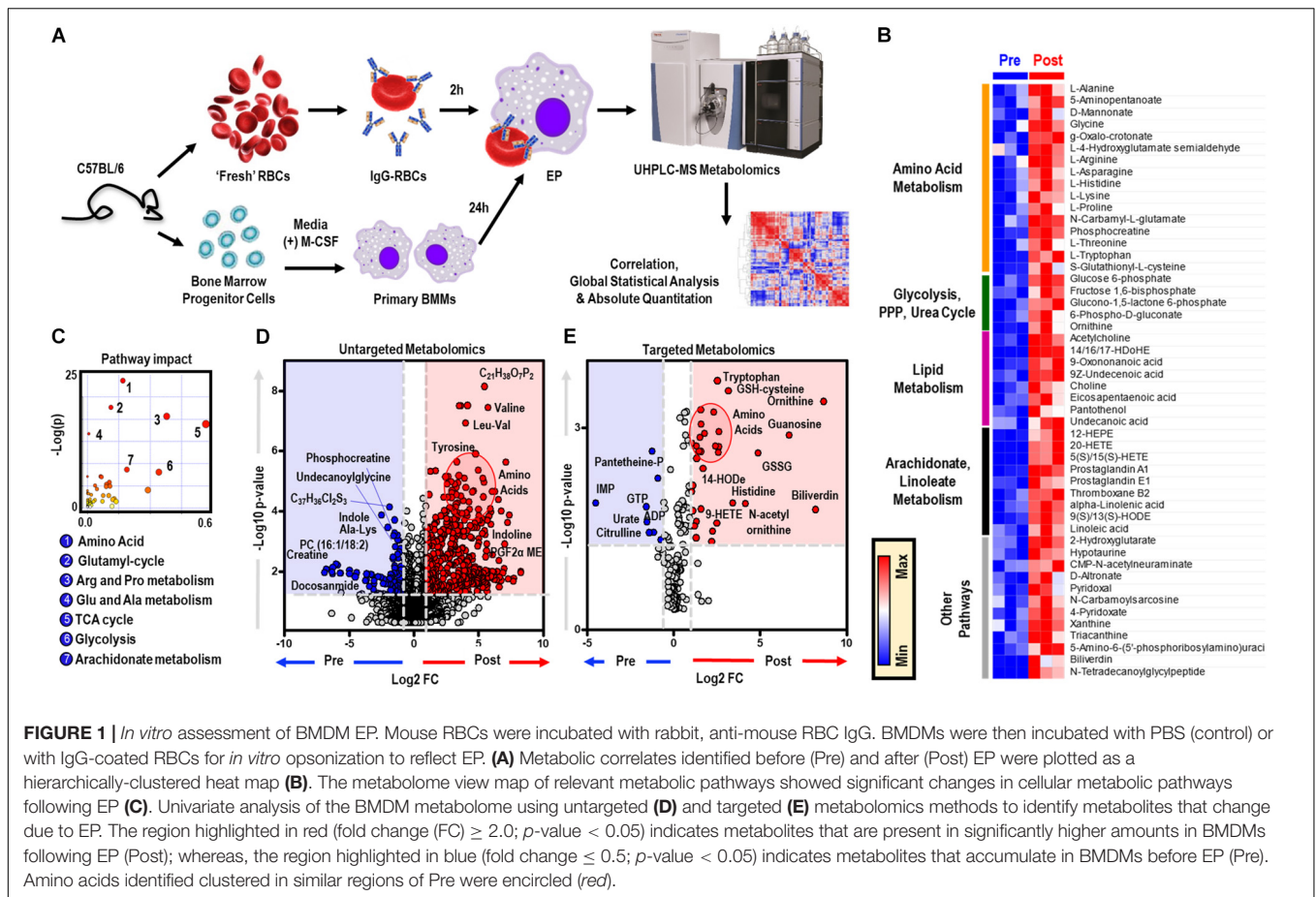
Statistical Analysis

Statistical (i.e., *t*-test, ANOVA, linear regression and Spearman correlations) and multivariate [i.e., principal component analysis (PCA), partial least squares-discriminant analysis (PLS-DA), and hierarchical clustering analysis (HCA)] analyses, heat maps, and graphs were performed and prepared using GraphPad Prism 5.0 (GraphPad Software, Inc., La Jolla, CA, United States), Morpheus (Broad Institute; Boston, MA, United States), and MetaboAnalyst 4.0 (Chong et al., 2018).

RESULTS

EP Induces Extensive Metabolic Reprogramming of BMDMs

To elucidate the metabolic phenotype of macrophages following EP, BMDMs were isolated from C57BL/6 mice and incubated with IgG-opsonized RBCs for 2 h at 37°C. Extracellular media (supernatants) and cell pellets were collected for metabolomics (Figure 1A) and analyzed using untargeted (Figure 1D) and targeted (Figure 1E) mass spectrometry methods. In Supplementary Figures S1A,B, we provide an overview of the untargeted metabolomics workflow and volcano plot from the data generated through this approach; in addition, we report absolute quantification in cells and supernatants are provided in Supplementary Figures S1C,D for of amino acids, and Supplementary Figures S1E,F glycolytic metabolites and oxylipins. An extensive report of the metabolomics data is provided in [Supplementary Table S1 and Supplementary Figures S1A,B, *Untargeted*, *Targeted* (5 MM), and *Global* (5 MM) Tabs]. Similarly, cell pellet metabolomics analyses were performed on BMDMs incubated with IgG to ensure that changes to BMDM metabolome were due to ingestion of IgG-opsonized RBCs and not to IgG binding alone (Supplementary Figure S2 and extensively reported in Supplementary Table S2). Increased levels of tryptophan, flavin mononucleotide (FMN, $p = 0.0002$), maltose ($p = 0.0002$), and 2-methyleneglutarate (2-MG, $p = 0.0021$) were noted in BMDMs that were incubated with IgG and are indicative of reprogramming of riboflavin, sugar, and C₅-dibasic acid metabolism (*data not shown*). Although this

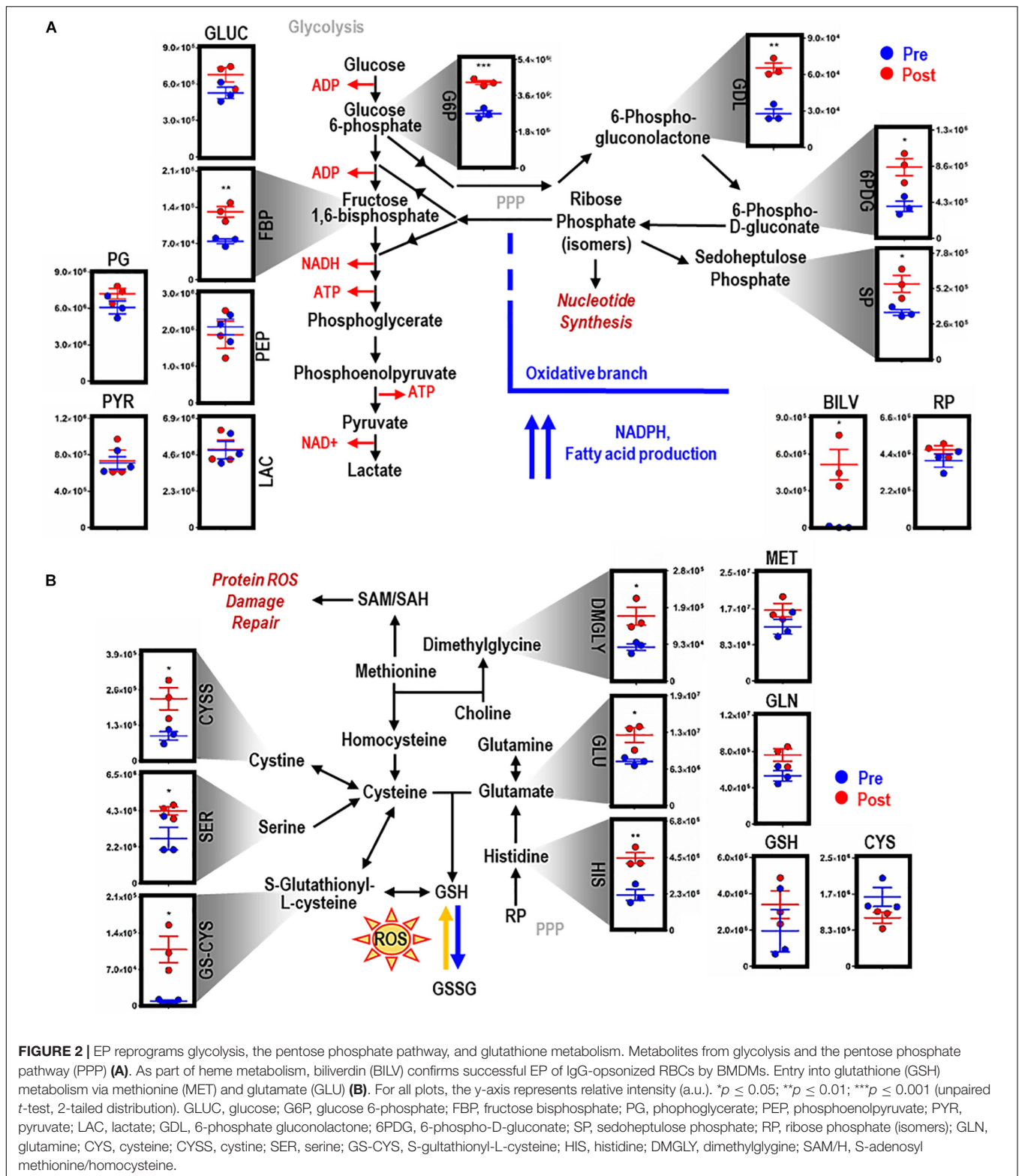


could have implications for macrophage effector function, similar to what has been reported for dendritic cell activation by Toll-like receptor signaling (Thwe et al., 2017), these results will not be discussed further except in the context of comparing particular metabolites found to be involved in EP-mediated metabolic reprogramming. Following EP, BMDMs were characterized by substantial increases in hundreds of metabolites (Figures 1D,E), some of which are plotted in the heat maps of Figures 1B, 5A. Specifically, enrichment was observed in pathways involved in amino acid and fatty acid metabolism, the Krebs cycle [also referred to as the tricarboxylate acid (TCA) cycle], and arachidonate metabolism (pathway leading to eicosanoid and oxylipin production; Figure 1C).

EP Increases Metabolites Involved in PPP and GSH Metabolism

EP promoted significant accumulation of early [i.e., glucose 6-phosphate (G6P), $p = 0.009$; fructose biphosphate (FBP), $p = 0.0078$] but not late (e.g., pyruvate (PYR), lactate (LAC)] glycolytic metabolites (Figure 2A). Additionally, following EP, intermediates of the oxidative [i.e., 6-phosphogluconolactone (GDL), $p = 0.0027$; 6-phosphogluconate (6PDG), $p = 0.0170$] and non-oxidative [i.e., sedoheptulose phosphate (SP), $p = 0.0109$]

branches of the PPP increased significantly (Figure 2A). These results suggested a slower flux through glycolysis and enhanced PPP activation. To test this hypothesis, tracing experiments were performed by incubating BMDMs with $^{13}\text{C}_6$ -glucose 1 h prior to and during EP (Figure 3). These results indicated that $^{13}\text{C}_5$ -ribose phosphate and pentose phosphate isobaric isomers were exclusively labeled from glucose taken up *de novo* during EP (Figure 3B, green) or from endogenous glucose already in the macrophage prior to EP (Figure 3B, red), but not from the RBCs themselves (Figure 3B, blue). This suggests that RBC-derived cytosolic sugars do not participate in fueling this activation of glycolysis or the PPP. PPP activation is consistent with (i) increased oxidant stress resulting from phagocytosis of iron-loaded RBCs; and (ii) increased flux through NADPH-generating pathways to fuel NADPH oxidase-dependent ROS production to target the engulfed cell via radical attack (Xu et al., 2016). Consistent with increased oxidant stress, decreases in free reduced cysteine and significant increases in oxidized cysteine disulfide [cystine (CYSS), $p = 0.0348$] and cysteine glutathione disulfide [S-glutathionyl-L-cysteine (GS-CYS), $p = 0.0110$] were noted (Figure 2B). Further, higher levels of histidine (HIS, $p = 0.0091$), glutamate (GLU, $p = 0.0283$), methionine, serine (SER, $p = 0.0392$), and dimethylglycine (DMGLY, $p = 0.0308$) indicate alterations of glutathione and sulfur homeostasis



and one-carbon metabolism, which are involved in repairing oxidant protein damage (Reisz et al., 2018; **Figure 2B** and **Supplementary Figure S1C**). Importantly, these metabolites did

not increase when BMDMs were incubated with IgG alone (the subset of significant metabolites with pathways noted in **Supplementary Figures S2C,D**).

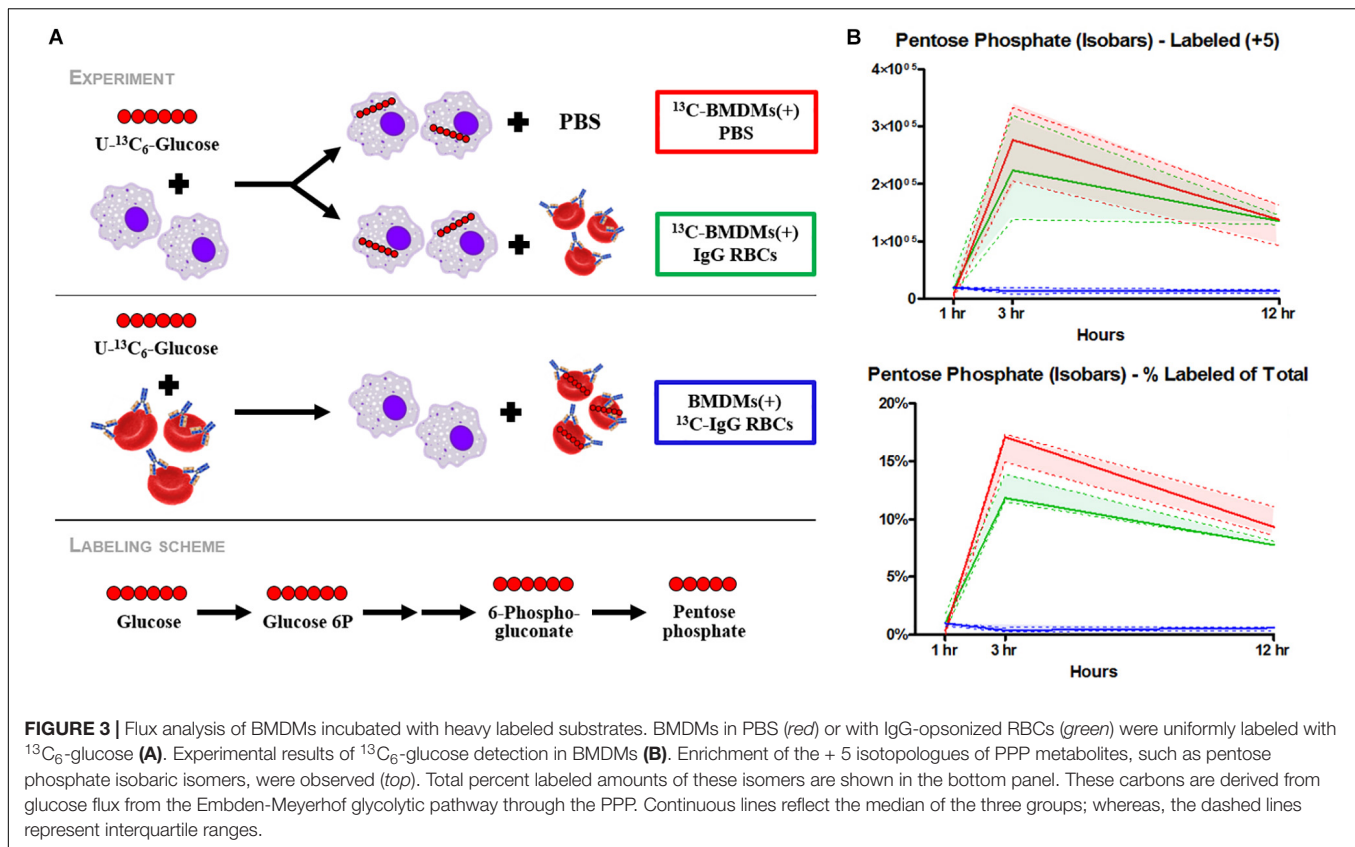


FIGURE 3 | Flux analysis of BMDMs incubated with heavy labeled substrates. BMDMs in PBS (red) or with IgG-opsonized RBCs (green) were uniformly labeled with ¹³C₆-glucose (A). Experimental results of ¹³C₆-glucose detection in BMDMs (B). Enrichment of the + 5 isotopologues of PPP metabolites, such as pentose phosphate isobaric isomers, were observed (top). Total percent labeled amounts of these isomers are shown in the bottom panel. These carbons are derived from glucose flux from the Embden-Meyerhof glycolytic pathway through the PPP. Continuous lines reflect the median of the three groups; whereas, the dashed lines represent interquartile ranges.

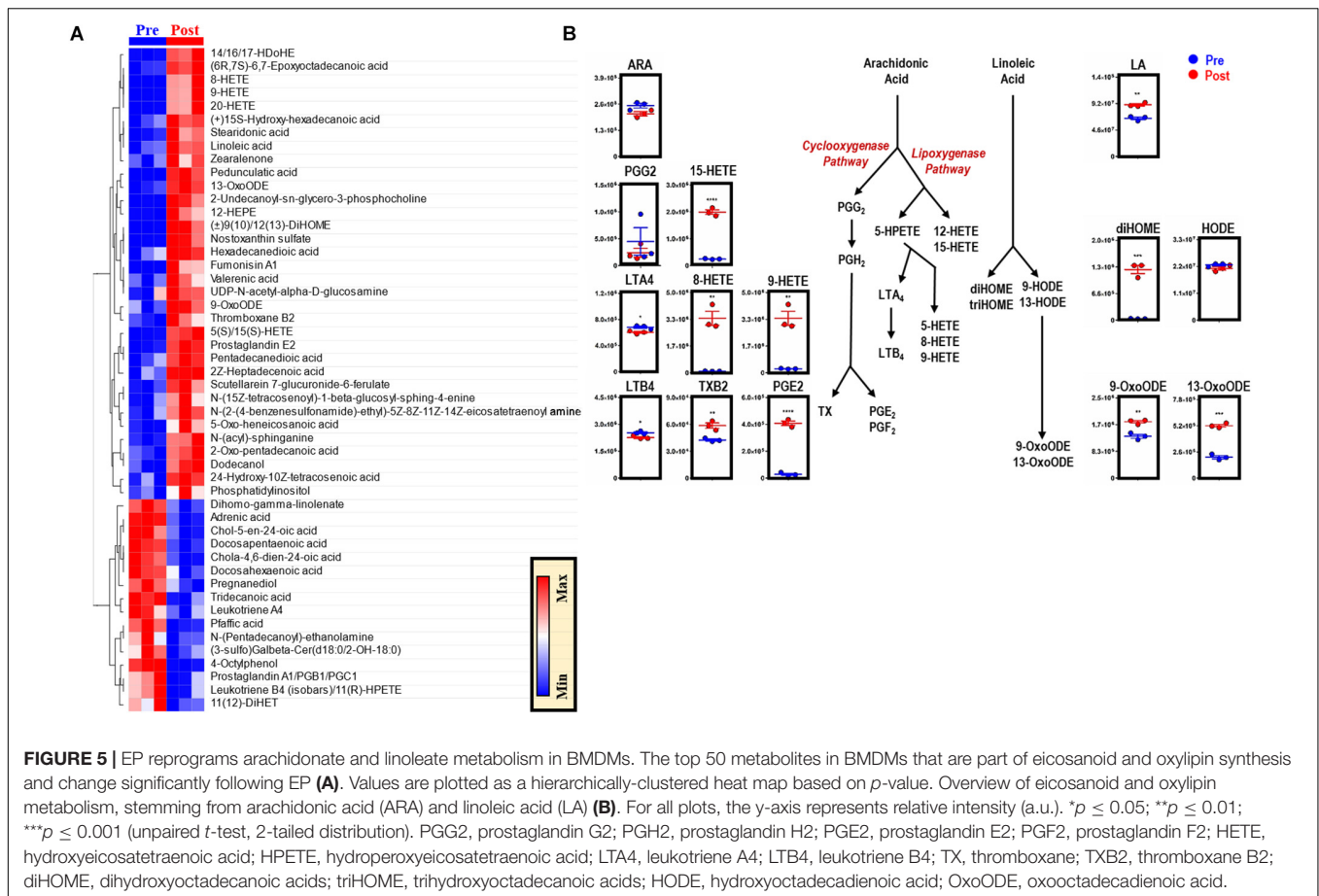
EP Promotes Purine Oxidation and Dysregulation of Mitochondrial Metabolism

Consistent with dysregulated glutathione homeostasis, increased purine oxidation was observed in macrophages upon EP, as indicated by ATP breakdown and increases in oxidation products, including inosine, hypoxanthine (HPX, $p = 0.0377$), and xanthine (XAN, $p = 0.0088$) (Figure 4A). HPX and XAN did not accumulate upon incubation of BMDMs with IgG alone (Supplementary Figure S2C). Purine oxidation is tied to mitochondrial metabolism via salvage reactions fueled by aspartate consumption and fumarate generation. Of note, higher levels of intracellular aspartate (ASP, $p = 0.0332$), but not fumarate, were observed in macrophages upon EP. Further, increases in α -ketoglutarate (α KG, $p = 0.0048$), 2-hydroxyglutarate (2HG, $p = 0.0017$), and itaconate were detected after EP in the absence of increases in late carboxylic acid intermediates (e.g., succinate, fumarate; Figure 4B). Hence, significant decreases in succinate to itaconate ratios (SUCC/ITA, $p = 0.0215$) were noted (Figure 4B, boxed in red). Consistent with decreased NO synthase (NOS) activity and increased arginase activity following EP, increases in free arginine (ARG, $p = 0.0173$) and ornithine (ORN, $p = 0.0074$), but not citrulline or polyamines (spermidine), were noted (Figure 4B). Lastly, upregulation of ALA synthase, due to an intracellular bolus of iron and heme in BMDMs during EP, was confirmed by a significant increase of ALA ($p = 0.0344$; Figure 4B). Increased levels of these metabolites

were not observed when BMDMs were incubated with IgG alone (Supplementary Figure S2E, subset of significant metabolites).

EP Induces Significant Increases in Prostaglandins and Oxylipins

Phospholipid hydrolysis generates free fatty acids, including arachidonate (the direct precursor of eicosanoids), thereby directly modulating inflammation, immunity, and other signaling pathways (Esser-von Bieren, 2017). Dysregulation of intracellular redox metabolism can result in increased peroxidation of macrophage membrane-derived lipids. Following EP, macrophages are exposed to a bolus of RBC membrane-derived lipids that are susceptible to lipid peroxidation and iron stores that can activate cyclooxygenases (COXs) and generate proinflammatory eicosanoid derivatives (Youssef et al., 2018). Therefore, lipidomics analyses were performed to investigate the production of eicosanoids and oxylipins in BMDMs after EP [Figure 5 and extensively reported in Supplementary Table S1, Global (17MM) Tab]. Decreases in arachidonic acid were found, accompanied by decreases in leukotrienes and significant increases in thromboxane B2 (TXB2, $p = 0.0070$), prostaglandin E2 (PGE2, $p < 0.0001$), and hydroxyeicosatrienate (HETE) derivatives [5(S)/15(S)-HETE, $p < 0.0001$; 8-HETE, $p = 0.0016$; 9/20-HETE, $p = 0.0019$] (Figure 5). Further, increases in linoleic acid (LA, $p = 0.0013$) were accompanied by accumulation of dihydroxyoctadecenate (diHOME, $p = 0.0003$) and oxooctadecadienates (9-oxoODE, $p = 0.0032$; 13-oxoODE,



p = 0.0001), without increases in hydroxyoctadecadienate (HODE) (Figure 5).

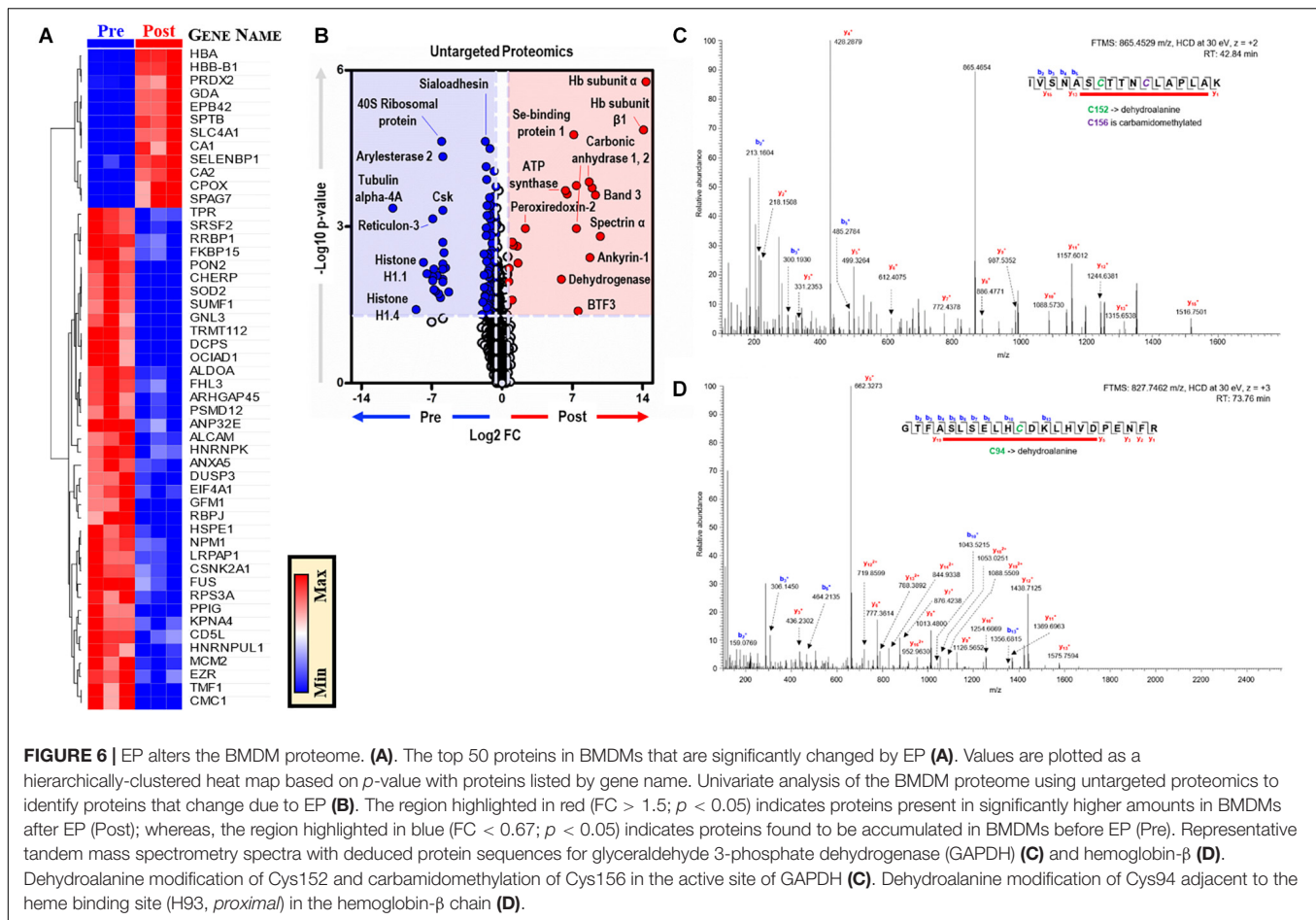
EP Modulates the Protein Landscape, Including Modifications of Key Metabolic Enzymes

Proteomics analyses of BMDMs, before and after EP, identified ~3,000 unique proteins (Supplementary Table S3). Unsupervised analyses, including PLS-DA, identified significant effects of EP on the BMDM proteome, contributing to ~51% of the total variance (Supplementary Figure S2A). Top proteins are presented in a PLS-DA variable importance in projection (VIP) plot (Supplementary Figures S3A,B) and in heat maps of Supplementary Figure S3C (top 15) and Figure 6A (top 50). EP induced increases in RBC-derived protein components (e.g., hemoglobin, band 3, spectrin, ankyrin, selenium-binding protein, peroxiredoxin 2) in BMDMs (Figure 6B). Notably, the functional cysteine (Cys) residues of RBC-derived proteins were irreversibly oxidized to dehydroalanine, including Cys94 of hemoglobin-β and Cys152 of glyceraldehyde 3-phosphate dehydrogenase (GAPDH) (Figures 6C,D). Conversely, cytoskeletal components (e.g., tubulin 4A), ribosomal proteins (e.g., 40S ribosomal protein), mitochondrial components, and nuclear components (e.g., histones) were decreased after EP (Figure 6B). No

significant changes in interleukins, interferons, or interferon-dependent proteins were observed after EP. Notably, the terminal oxidase in mitochondrial electron transport (COX5A) increased significantly after EP, which is consistent with the alterations to mitochondrial metabolism discussed previously.

DISCUSSION

Metabolic reprogramming is critical to the immune response and contributes significantly to macrophage effector function (Martinez and Gordon, 2014). Macrophage immunometabolism is affected by various factors, including cytokines (Martinez and Gordon, 2014), complement components (Bohlsón et al., 2014), pathogen-derived molecules (e.g., LPS) (Tannahill et al., 2013), and environmental stimuli [e.g., diet, Ji et al., 2012, and dietary antioxidants, such as pyrroloquinoline quinone (Van den Bossche et al., 2017; Friedman et al., 2018)]. Reprogramming of macrophage metabolism contributes to the etiopathogenesis of several diseases, including pulmonary hypertension (Pugliese et al., 2017; D'Alessandro et al., 2018), age-related chronically inflammatory diseases (Oishi and Manabe, 2016; Parisi et al., 2018), neurodegenerative diseases (Peruzzotti-Jametti et al., 2018), and inflammatory complications following ischemia and reperfusion (Chouchani et al., 2014; Huen and Cantley, 2015).



However, limited knowledge is available about the impact of phagocytic activity and increased heme-iron burden on macrophage metabolism, which is crucial for pathogen defense mechanisms and general system homeostasis.

The present study investigated the impact of EP on macrophage metabolism and revealed that EP activates a series of pathways consistent with polarization toward the M2 metabolic phenotype, including those that support the generation of reducing cofactor NADPH. We address the question of whether these metabolic shifts were fueled by catabolism of RBC-derived substrates through glucose tracing experiments. Interestingly, EP fuels the PPP primarily by using glucose from extracellular sources or from macrophage reserves, rather than from RBC-derived sugar moieties. Whereas PPP activation in other non-phagocytic cell types typically counteracts oxidant stress, macrophages specifically use this pathway to produce ROS by, for example, upregulating nicotinamide adenine dinucleotide phosphate oxidase (NOX) 1 and 2 expression (Xu et al., 2016). Through increased NOX catalytic activity, superoxide generation enhances ROS production by macrophages, thereby supporting phagocytic activity during microbial infections and the use of heme-iron for electron transport across biological membranes (Xu et al., 2016). Further, NOX-generated ROS increase proteolytic attack of phagocytosed cellular components,

which correlates with the redox proteomics analysis results presented herein. Although we expected to observe significant increases of RBC-derived proteins in macrophages after EP, these proteins were rapidly targeted by irreversible oxidation within 1 h. A key example was the peroxidation of Cys94 of hemoglobin- β , which participates in recycling oxidized thiols of peroxiredoxins in mature RBCs and is progressively oxidized in RBCs during aging *in vivo* and *in vitro* (Harper et al., 2015; Wither et al., 2016). Irreversible oxidation of hemoglobin- β Cys94 and of active-site Cys152 of GAPDH suggests that RBC-derived enzymes are rapidly inactivated upon EP. Since Cys152 oxidation of GAPDH is required for catalysis, redox modulation of this residue is sufficient for mediating a metabolic switch from glycolysis to the PPP by limiting fluxes downstream of glyceraldehyde 3-phosphate (Reisz et al., 2016, 2018). Because no significant increases in late glycolysis and lactate production were observed in BMDMs following EP, we cannot exclude the possibility that the redox changes detected of the reactive thiol of Cys152 also targeted the endogenous (macrophage) enzyme. In RBCs, GAPDH membrane localization is associated with binding to the N-terminus of band 3, inhibiting glycolysis to promote PPP flux in response to oxidant challenges (Puchulu-Campanella et al., 2013), whereas subcellular GAPDH relocation in macrophages

plays unexpected moonlighting functions (Chauhan et al., 2017). Clustering of band 3 can prime RBC clearance, since they are recognized by natural antibodies of the IgG isotype, triggering complement activation via the classical pathway and enhancement of EP via macrophage complement receptors 1 (CD35) and 3 (CD11b/CD18), and Fc receptors (Lutz, 2004; Arese et al., 2005; Kay, 2005; Klei et al., 2017). Macrophages exposed to increased levels of iron then relocate GAPDH to the membrane, where it interacts with transferrin and serves as a *de facto* transferrin or plasminogen receptor to regulate iron uptake and fibrinolysis (Polati et al., 2012; Chauhan et al., 2017). When not engaged in glycolysis, GAPDH can bind TNF- α mRNA in monocytes to repress the production of this inflammatory cytokine post-transcriptionally (Van den Bossche et al., 2017). Interestingly, though the mechanism that regulates the metabolic shift to the PPP in the phagocytic cell is not better defined in this study, the steady state data and tracing experiments are suggestive of a potential bottleneck downstream to fructose 1,6-bisphosphate at the level of the glycolytic enzyme aldolase. Though speculative at this stage, it is interesting to note that the N-term of RBC-specific band 3 also binds to and inhibits aldolase (other than GAPDH), suggestive that the proteolysis-derived components of the phagocytosed RBC could cross-regulate the metabolism of the macrophage.

Krebs cycle rewiring has profound implications for macrophage effector function and is intimately involved in the remodeling necessary for supporting biosynthetic and bioenergetic requirements (Ryan and O'Neill, 2017). This pathway is disrupted during macrophage activation by inflammatory stimuli and leads to the accumulation of various metabolites, including succinate and citrate (Jha et al., 2015; Lampropoulou et al., 2016; Ryan and O'Neill, 2017; Williams and O'Neill, 2018; Yu et al., 2019). Although succinate and itaconate levels were not significantly elevated before or after EP, a significant SUCC/ITA ratio ($p = 0.0215$) was observed in BMDMs following RBC ingestion, suggesting that the balance between these two metabolites is regulated by EP. Notably, the lack of succinate accumulation following EP is consistent with inhibition of proinflammatory cascades (i.e., stabilization of HIF1 α impairs production of downstream targets, such as IL-1 β ; Selak et al., 2005; Tannahill et al., 2013). Other metabolites that influence prolyl hydroxylases to regulate HIF1 α stability include α KG (the precursor to succinate) and fumarate (Boulahbel et al., 2009). While fumarate levels did not increase significantly following EP, α KG, and 2HG (a reversible derivative of α KG) accumulated significantly. Notably, α KG also plays a critical role in epigenetic reprogramming of macrophages (Liu et al., 2017; e.g., it drives Jumonji-Domain Containing Protein 3-dependent epigenetic changes to modulate macrophage effector function) (Diskin and Palsson-McDermott, 2018) whereas, 2HG impairs the activity of α KG-dependent dioxygenases associated with important cellular pathways, such as DNA repair (Ye et al., 2018).

In inflammatory macrophages, HIF1 α stabilization can also be achieved via S-nitrosylation mediated by NO availability

(Olson and van der Vliet, 2011). But in M2 macrophages, NOS-mediated NO synthesis is prevented by arginine consumption by enzymes such as Arg-1 (Rath et al., 2014). Consistent with increased arginase activity at the expense of NOS activity, EP significantly increased arginine and ornithine levels, but not citrulline. Since RBCs carry both NOS and arginase (D'Alessandro et al., 2019), it is possible that these enzymes could interfere with these pathways in macrophages upon EP. However, NOS is more redox sensitive (Forstermann and Sessa, 2012) and is readily inactivated by EP-induced oxidant stress. Future tracing experiments with $^{13}\text{C}^{15}\text{N}$ -arginine in an RBC-specific arginase knockout mouse could test this hypothesis.

Macrophages that have undergone EP are exposed to the cytosolic and membrane lipidome of the opsonized RBCs. The M2 metabolic phenotype is associated with an increased reliance on mitochondrial metabolism and fatty acid catabolism (Nomura et al., 2016; Remmerie and Scott, 2018). Fatty acid oxidation (FAO) enables subsequent conversion of mitochondrial fatty acids into numerous products, such as acetyl-coenzyme A (acetyl-CoA), NADH, and FADH₂, which can be used by the cell to generate energy (Remmerie and Scott, 2018). EP promoted consumption of CoA precursors (e.g., pantothenol phosphate) and accumulation of free fatty acids in the absence of significant acyl-conjugated carnitine accumulation. Heme catabolism leads to the activation of anti-inflammatory cascades (e.g., HO-1 activation; Naito et al., 2014), but can also prompt the generation of proinflammatory lipid mediators. Significant increases in intracellular heme catabolites, such as biliverdin (BILV, $p = 0.0151$), following EP confirmed activation of heme catabolism. Further, several metabolites involved in ARA and LA metabolism increased significantly, which could be aided by various hemoproteins (e.g., COXs). During the inflammatory phase following injury or infection, macrophages are natural reservoirs of COX-2 and prostaglandins, and this pathway is, indeed, activated by iron-triggered ferroptotic cascades in response to iron overload in macrophages following phagocytosis of transfused, storage-damaged RBCs (Youssef et al., 2018). Consistent with this, EP-induced increases of specific oxylipins (i.e., prostaglandins, HETEs, diOMEs, and oxoODEs, but not leukotrienes or HODEs). It is intriguing to speculate whether pathological EP, in the context of chronic inflammatory diseases and aging (e.g., in the context of inflammaging-induced anemia; Ferrucci and Balducci, 2008), may excessively activate ferroptotic cascades, thereby exacerbating the risk of bacterial infection. Further, this may be clinically relevant for transfusion recipients of stored RBCs, since REM-mediated clearance is expected to be enhanced by the RBC "storage lesion" (e.g., increased PS exposure, decreased exposure of CD47 (a "do not eat me" signal; Burger et al., 2012a,b), and decreased deformability) (D'Alessandro et al., 2015; Takimoto et al., 2019). This is significant if one considers that ~25% of transfused RBCs can be cleared within 24 h post-transfusion and there are ~5 million transfusion recipients annually in the United States.

Most immunometabolism studies to date rely on LPS or cytokine-dependent stimulation of macrophages, and the literature describing the metabolic impact of phagocytosis itself is scarce to non-existent. Thus, this study provides the first metabolic description of macrophages following ingestion of opsonized RBCs. Before summarizing our main conclusions, we would like to highlight some of the limitations of this study: first of all, the *ex vivo* nature of the study and the use of mouse BMDMs may not necessarily recapitulate the phenomenon of EP *in vivo* by tissue-specific residential macrophages in mice or humans; in addition, the lack of potentially relevant controls (e.g., phagocytosis of IgG-coated latex beads or C3b complement-mediated phagocytosis) or the use of other mouse strains than C57BL/6 mice may have differentially impacted our findings, at least to the extent different mouse strains have been reported to differ in iron reduction and homeostasis (Howie et al., 2019) – a key component of EP (Youssef et al., 2018). Acknowledging these limitations, here we report that EP induces changes in the macrophage metabolome that are consistent with polarization toward an M2 metabolic phenotype. One caveat is that these experiments focus on a metabolomic assessment of BMDMs ingesting IgG-opsonized RBCs, or being incubated with IgG, *in vitro*; thus, transcriptional and flow cytometric data from experiments performed *in vivo* are necessary to confirm the apparent upregulation and/or downregulation of the gene products identified from our proteomic analysis. Additionally, no direct interventions were tested to determine whether genetic or pharmacological manipulation could identify which specific, EP-modulated, metabolic pathways are critical for macrophage reprogramming toward a M2 metabolic phenotype. Indeed, the specific pathways identified differ when macrophages ingest other particles (i.e., IgG-opsonized bacteria, viruses, or apoptotic cells) or when Fcγ-receptors are ligated by immune complexes. However, we do show that incubation of BMDMs with IgG alone does not induce metabolic reprogramming similar to that mediated by EP. Future studies are necessary to confirm these results in more physiologically relevant contexts *in vivo*, such as during hemolytic transfusion reactions or autoimmune hemolytic anemia, or in settings of splenic (and hepatic) REM ingestion of senescent RBCs, malaria-infected RBCs, or transfused storage-damaged RBCs.

DATA AVAILABILITY STATEMENT

The proteomic data has been deposited into the Proteome XChange database (accession: PXD017788).

REFERENCES

- Alayash, A. I., Patel, R. P., and Cashion, R. E. (2001). Redox reactions of hemoglobin and myoglobin: biological and toxicological implications. *Antioxid. Redox Signal.* 3, 313–327. doi: 10.1089/152308601300185250
- Alsultan, A. I., Seif, M. A., Amin, T. T., Naboli, M., and Alsuliman, A. M. (2010). Relationship between oxidative stress, ferritin and insulin resistance in sickle cell disease. *Eur. Rev. Med. Pharmacol. Sci.* 14, 527–538.

ETHICS STATEMENT

All procedures were approved by the Institutional Animal Care and Use Committee at Columbia University (New York City, NY, United States).

AUTHOR CONTRIBUTIONS

AD'A, SS, LY, and AC conceived and designed the metabolomics studies. AC performed the metabolic analyses of all macrophage experiments. LY performed the *in vitro* EP assay and U-¹³C₆-glucose tracing experiments with the macrophages. AD'A contributed to the metabolic analysis of the tracing experiments. MD performed the proteomics analysis, and AD'A, JR, AC, and KCH contributed to the analysis of the proteomic data. NP and CM performed the *in vitro* IgG assay with the macrophages. AC and AD'A drafted the first version of the manuscript, and AC, JR, and AD'A prepared all figures. All co-authors contributed to preparing the final manuscript.

FUNDING

The research reported herein was supported by NIH T32 AI106711 (LY), F31 HL134284 (LY), NIH R01 HL115557 (SS), R01 HL133049 (SS), R01 HL148151 (SS, AD'A, MK, and JZ), RM1GM131968 (AD'A and KCH), R01 HL146442, R01 HL149714 (AD'A, JZ, and KCH), NHLBI R01 HL149714 (AD'A), and R21 HL150032 (AD'A), and the Boettcher Webb-Waring Investigator Award the Shared Instrument grant from the NIH Office of the Director (S10OD021641) (AD'A and KCH). AC was supported by the NSF GRFP 1553798. Any opinions, findings, conclusions or recommendations expressed are those of the authors and do not necessarily reflect the views of the NIH or NSF.

ACKNOWLEDGMENTS

We would like to thank Dr. B Wojczyk for his help in the initial stages of developing the *in vitro* erythrophagocytosis assay.

SUPPLEMENTARY MATERIAL

The Supplementary Material for this article can be found online at: <https://www.frontiersin.org/articles/10.3389/fphys.2020.00396/full#supplementary-material>

- Arese, P., Turrini, F., and Schwarzer, E. (2005). Band 3/complement-mediated recognition and removal of normally senescent and pathological human erythrocytes. *Cell. Physiol. Biochem.* 16, 133–146. doi: 10.1159/000089839
- Barr, J. D., Chauhan, A. K., Schaeffer, G. V., Hansen, J. K., and Motto, D. G. (2013). Red blood cells mediate the onset of thrombosis in the ferric chloride murine model. *Blood* 121, 3733–3741. doi: 10.1182/blood-2012-11-468983
- Belanger, A. M., Keggi, C., Kanas, T., Gladwin, M. T., and Kim-Shapiro, D. B. (2015). Effects of nitric oxide and its congeners on sickle red blood cell deformability. *Transfusion* 55, 2464–2472. doi: 10.1111/trf.13134

- Belcher, J. D., Chen, C., Nguyen, J., Zhang, P., Abdulla, F., Nguyen, P., et al. (2017). Control of oxidative stress and inflammation in sickle cell disease with the Nrf2 activator dimethyl fumarate. *Antioxid. Redox Signal.* 26, 748–762. doi: 10.1089/ars.2015.6571
- Bohlson, S. S., O'connor, S. D., Hulsebus, H. J., Ho, M. M., and Fraser, D. A. (2014). Complement, c1q, and c1q-related molecules regulate macrophage polarization. *Front. Immunol.* 5:402. doi: 10.3389/fimmu.2014.00402
- Boulahbel, H., Duran, R. V., and Gottlieb, E. (2009). Prolyl hydroxylases as regulators of cell metabolism. *Biochem. Soc. Trans.* 37, 291–294. doi: 10.1042/BST0370291
- Brown, C. D., Ghali, H. S., Zhao, Z., Thomas, L. L., and Friedman, E. A. (2005). Association of reduced red blood cell deformability and diabetic nephropathy. *Kidney Int.* 67, 295–300. doi: 10.1111/j.1523-1755.2005.00082.x
- Burger, P., De Korte, D., Van Den Berg, T. K., and Van Bruggen, R. (2012a). CD47 in erythrocyte ageing and clearance – the Dutch point of view. *Transfus. Med. Hemother.* 39, 348–352. doi: 10.1159/000342231
- Burger, P., Hilarius-Stokman, P., De Korte, D., Van Den Berg, T. K., and Van Bruggen, R. (2012b). CD47 functions as a molecular switch for erythrocyte phagocytosis. *Blood* 119, 5512–5521. doi: 10.1182/blood-2011-10-386805
- Cao, J. Y., and Dixon, S. J. (2016). Mechanisms of ferroptosis. *Cell. Mol. Life Sci.* 73, 2195–2209. doi: 10.1007/s00018-016-2194-1
- Caspary, E. A., Sewell, F., and Field, E. J. (1967). Red blood cell fragility in multiple sclerosis. *Br. Med. J.* 2, 610–611. doi: 10.1136/bmj.2.5552.610
- Catala, A., Culp-Hill, R., Nemkov, T., and D'alessandro, A. (2018). Quantitative metabolomics comparison of traditional blood draws and TAP capillary blood collection. *Metabolomics* 14:100. doi: 10.1007/s11306-018-1395-z
- Chauhan, A. S., Kumar, M., Chaudhary, S., Patidar, A., Dhiman, A., Sheokand, N., et al. (2017). Moonlighting glycolytic protein glyceraldehyde-3-phosphate dehydrogenase (GAPDH): an evolutionarily conserved plasminogen receptor on mammalian cells. *FASEB J.* 31, 2638–2648. doi: 10.1096/fj.201600982R
- Chong, J., Soufan, O., Li, C., Caraus, I., Li, S., Bourque, G., et al. (2018). MetaboAnalyst 4.0: towards more transparent and integrative metabolomics analysis. *Nucleic Acids Res.* 46, W486–W494. doi: 10.1093/nar/gky310
- Chouchani, E. T., Pell, V. R., Gaude, E., Aksentijevic, D., Sundier, S. Y., Robb, E. L., et al. (2014). Ischaemic accumulation of succinate controls reperfusion injury through mitochondrial ROS. *Nature* 515, 431–435. doi: 10.1038/nature13909
- Curi, R., De Siqueira Mendes, R., De Campos Crispin, L. A., Norata, G. D., Sampaio, S. C., and Newsholme, P. (2017). A past and present overview of macrophage metabolism and functional outcomes. *Clin. Sci. (Lond.)* 131, 1329–1342. doi: 10.1042/CS20170220
- D'alessandro, A., El Kasm, K. C., Plecitan-Hlavata, L., Jezek, P., Li, M., Zhang, H., et al. (2018). Hallmarks of pulmonary hypertension: mesenchymal and inflammatory cell metabolic reprogramming. *Antioxid. Redox Signal.* 28, 230–250. doi: 10.1089/ars.2017.7217
- D'alessandro, A., Kriebardis, A. G., Rinalducci, S., Antonelou, M. H., Hansen, K. C., Papassideri, I. S., et al. (2015). An update on red blood cell storage lesions, as gleaned through biochemistry and omics technologies. *Transfusion* 55, 205–219. doi: 10.1111/trf.12804
- D'alessandro, A., Reisz, J. A., Zhang, Y., Gehrke, S., Alexander, K., Kanas, T., et al. (2019). Effects of aged stored autologous red blood cells on human plasma metabolome. *Blood Adv.* 3, 884–896. doi: 10.1182/bloodadvances.2018029629
- de Back, D. Z., Kostova, E. B., Van Kraaij, M., Van Den Berg, T. K., and Van Bruggen, R. (2014). Of macrophages and red blood cells; a complex love story. *Front. Physiol.* 5:9. doi: 10.3389/fphys.2014.00009
- Diskin, C., and Palsson-McDermott, E. M. (2018). Metabolic modulation in macrophage effector function. *Front. Immunol.* 9:270. doi: 10.3389/fimmu.2018.00270
- Dixon, S. J., Lemberg, K. M., Lamprecht, M. R., Skouta, R., Zaitsev, E. M., Gleason, C. E., et al. (2012). Ferroptosis: an iron-dependent form of nonapoptotic cell death. *Cell* 149, 1060–1072. doi: 10.1016/j.cell.2012.03.042
- Esser-von Bieren, J. (2017). Immune-regulation and -functions of eicosanoid lipid mediators. *Biol. Chem.* 398, 1177–1191. doi: 10.1515/hsz-2017-0146
- Ferrucci, L., and Balducci, L. (2008). Anemia of aging: the role of chronic inflammation and cancer. *Semin. Hematol.* 45, 242–249. doi: 10.1053/j.seminhematol.2008.06.001
- Forstermann, U., and Sessa, W. C. (2012). Nitric oxide synthases: regulation and function. *Eur. Heart J.* 33, 829–837. doi: 10.1093/eurheartj/ehr304
- Friedman, J. E., Dobrinskikh, E., Alfonso-Garcia, A., Fast, A., Janssen, R. C., Soderborg, T. K., et al. (2018). Pyrroloquinoline quinone prevents developmental programming of microbial dysbiosis and macrophage polarization to attenuate liver fibrosis in offspring of obese mice. *Hepatology* 67, 313–328. doi: 10.1002/hep4.1139
- Gaber, T., Strehl, C., and Buttgerit, F. (2017). Metabolic regulation of inflammation. *Nat. Rev. Rheumatol.* 13, 267–279. doi: 10.1038/nrrheum.2017.37
- Gkouvatsos, K., Papanikolaou, G., and Pantopoulos, K. (2012). Regulation of iron transport and the role of transferrin. *Biochim. Biophys. Acta* 1820, 188–202. doi: 10.1016/j.bbagen.2011.10.013
- Guida, C., Altamura, S., Klein, F. A., Galy, B., Boutros, M., Ulmer, A. J., et al. (2015). A novel inflammatory pathway mediating rapid hepcidin-independent hypoferremia. *Blood* 125, 2265–2275. doi: 10.1182/blood-2014-08-595256
- Haldar, M., Kohyama, M., So, A. Y., Kc, W., Wu, X., Briseno, C. G., et al. (2014). Heme-mediated SPI-C induction promotes monocyte differentiation into iron-recycling macrophages. *Cell* 156, 1223–1234. doi: 10.1016/j.cell.2014.01.069
- Harper, V. M., Oh, J. Y., Stapley, R., Marques, M. B., Wilson, L., Barnes, S., et al. (2015). Peroxiredoxin-2 recycling is inhibited during erythrocyte storage. *Antioxid. Redox Signal.* 22, 294–307. doi: 10.1089/ars.2014.5950
- Hod, E. A., Zhang, N., Sokol, S. A., Wojczyk, B. S., Francis, R. O., Ansaldi, D., et al. (2010). Transfusion of red blood cells after prolonged storage produces harmful effects that are mediated by iron and inflammation. *Blood* 115, 4284–4292. doi: 10.1182/blood-2009-10-245001
- Howie, H. L., Hay, A. M., de Wolski, K., Waterman, H., Lebedev, J., Fu, X., et al. (2019). Differences in Steap3 expression are a mechanism of genetic variation of RBC storage and oxidative damage in mice. *Blood Adv.* 3, 2272–2285. doi: 10.1182/bloodadvances.2019000605
- Huen, S. C., and Cantley, L. G. (2015). Macrophage-mediated injury and repair after ischemic kidney injury. *Pediatr. Nephrol.* 30, 199–209. doi: 10.1007/s00467-013-2726-y
- Jha, A. K., Huang, S. C., Sergushichev, A., Lampropoulou, V., Ivanova, Y., Loginicheva, E., et al. (2015). Network integration of parallel metabolic and transcriptional data reveals metabolic modules that regulate macrophage polarization. *Immunity* 42, 419–430. doi: 10.1016/j.immuni.2015.02.005
- Ji, Y., Sun, S., Xia, S., Yang, L., Li, X., and Qi, L. (2012). Short term high fat diet challenge promotes alternative macrophage polarization in adipose tissue via natural killer T cells and interleukin-4. *J. Biol. Chem.* 287, 24378–24386. doi: 10.1074/jbc.M112.371807
- Kay, M. (2005). Immunoregulation of cellular life span. *Ann. N. Y. Acad. Sci.* 1057, 85–111. doi: 10.1196/annals.1356.005
- Kelly, B., and O'Neill, L. A. (2015). Metabolic reprogramming in macrophages and dendritic cells in innate immunity. *Cell Res.* 25, 771–784. doi: 10.1038/cr.2015.68
- Klei, T. R., Meindert, S. M., Van Den Berg, T. K., and Van Bruggen, R. (2017). From the cradle to the grave: the role of macrophages in erythropoiesis and erythrophagocytosis. *Front. Immunol.* 8:73. doi: 10.3389/fimmu.2017.00073
- Kohyama, M., Ise, W., Edelson, B. T., Wilker, P. R., Hildner, K., Mejia, C., et al. (2009). Role for Spi-C in the development of red pulp macrophages and splenic iron homeostasis. *Nature* 457, 318–321. doi: 10.1038/nature07472
- Korolnek, T., and Hamza, I. (2015). Macrophages and iron trafficking at the birth and death of red cells. *Blood* 125, 2893–2897. doi: 10.1182/blood-2014-12-567776
- Kosman, D. J. (2010). Redox cycling in iron uptake, efflux, and trafficking. *J. Biol. Chem.* 285, 26729–26735. doi: 10.1074/jbc.R110.113217
- Kovtunovych, G., Eckhaus, M. A., Ghosh, M. C., Ollivierre-Wilson, H., and Rouault, T. A. (2010). Dysfunction of the heme recycling system in heme oxygenase 1-deficient mice: effects on macrophage viability and tissue iron distribution. *Blood* 116, 6054–6062. doi: 10.1182/blood-2010-03-272138
- Kuhn, V., Diederich, L., Keller, T. C. S. T., Kramer, C. M., Luckstadt, W., Panknin, C., et al. (2017). Red blood cell function and dysfunction: redox regulation, nitric oxide metabolism, anemia. *Antioxid. Redox Signal.* 26, 718–742. doi: 10.1089/ars.2016.6954
- Labonte, A. C., Tosello-Trampont, A. C., and Hahn, Y. S. (2014). The role of macrophage polarization in infectious and inflammatory diseases. *Mol. Cells* 37, 275–285. doi: 10.14348/molcells.2014.2374
- Lampropoulou, V., Sergushichev, A., Bambouskova, M., Nair, S., Vincent, E. E., Loginicheva, E., et al. (2016). Itaconate links inhibition of succinate

- dehydrogenase with macrophage metabolic remodeling and regulation of inflammation. *Cell Metab.* 24, 158–166. doi: 10.1016/j.cmet.2016.06.004
- Larsen, R., Gozzelino, R., Jeney, V., Tokaji, L., Bozza, F. A., Japiassu, A. M., et al. (2010). A central role for free heme in the pathogenesis of severe sepsis. *Sci. Transl. Med.* 2, 51ra71. doi: 10.1126/scitranslmed.3001118
- Li, P., Yin, Y. L., Li, D., Kim, S. W., and Wu, G. (2007). Amino acids and immune function. *Br. J. Nutr.* 98, 237–252.
- Liu, P. S., Wang, H., Li, X., Chao, T., Teav, T., Christen, S., et al. (2017). alpha-ketoglutarate orchestrates macrophage activation through metabolic and epigenetic reprogramming. *Nat. Immunol.* 18, 985–994. doi: 10.1038/ni.3796
- Lutz, H. U. (2004). Innate immune and non-immune mediators of erythrocyte clearance. *Cell. Mol. Biol. (Noisy-le-grand)* 50, 107–116.
- Martinez, F. O., and Gordon, S. (2014). The M1 and M2 paradigm of macrophage activation: time for reassessment. *F1000Prime Rep.* 6:13. doi: 10.12703/P6-13
- Meiser, J., Kramer, L., Sapcaru, S. C., Battello, N., Ghelfi, J., D'herouel, A. F., et al. (2016). Pro-inflammatory macrophages sustain pyruvate oxidation through pyruvate dehydrogenase for the synthesis of itaconate and to enable cytokine expression. *J. Biol. Chem.* 291, 3932–3946. doi: 10.1074/jbc.M115.676817
- Melamud, E., Vastag, L., and Rabinowitz, J. D. (2010). Metabolomic analysis and visualization engine for LC-MS data. *Anal. Chem.* 82, 9818–9826. doi: 10.1021/ac1021166
- Mills, E. L., Ryan, D. G., Prag, H. A., Dikovskaya, D., Menon, D., Zaslona, Z., et al. (2018). Itaconate is an anti-inflammatory metabolite that activates Nrf2 via alkylation of KEAP1. *Nature* 556, 113–117. doi: 10.1038/nature25986
- Mould, K. J., Barthel, L., Mohning, M. P., Thomas, S. M., Mccubbrey, A. L., Danhorn, T., et al. (2017). Cell origin dictates programming of resident versus recruited macrophages during acute lung injury. *Am. J. Respir. Cell Mol. Biol.* 57, 294–306. doi: 10.1165/rcmb.2017-0061OOC
- Nahrendorf, M., and Swirski, F. K. (2013). Monocyte and macrophage heterogeneity in the heart. *Circ. Res.* 112, 1624–1633. doi: 10.1161/circresaha.113.300890
- Naito, Y., Takagi, T., and Higashimura, Y. (2014). Heme oxygenase-1 and anti-inflammatory M2 macrophages. *Arch. Biochem. Biophys.* 564, 83–88. doi: 10.1016/j.abb.2014.09.005
- Nemkov, T., Reisz, J. A., Xia, Y., Zimring, J. C., and D'alessandro, A. (2018). Red blood cells as an organ? How deep omics characterization of the most abundant cell in the human body highlights other systemic metabolic functions beyond oxygen transport. *Expert Rev. Proteomics* 15, 855–864. doi: 10.1080/14789450.2018.1531710
- Noe, J. T., and Mitchell, R. A. (2019). Tricarballic acid cycle metabolites in the control of macrophage activation and effector phenotypes. *J. Leukoc. Biol.* 106, 359–367. doi: 10.1002/JLB.3RU1218-496R
- Nomura, M., Liu, J., Rovira, I., Gonzalez-Hurtado, E., Lee, J., Wolfgang, M. J., et al. (2016). Fatty acid oxidation in macrophage polarization. *Nat. Immunol.* 17, 216–217. doi: 10.1038/ni.3366
- Nonnenmacher, Y., and Hiller, K. (2018). Biochemistry of proinflammatory macrophage activation. *Cell. Mol. Life Sci.* 75, 2093–2109. doi: 10.1007/s00018-018-2784-1
- Oishi, Y., and Manabe, I. (2016). Macrophages in age-related chronic inflammatory diseases. *NPJ Aging Mech. Dis.* 2:16018. doi: 10.1038/npjamd.2016.18
- Olson, N., and van der Vliet, A. (2011). Interactions between nitric oxide and hypoxia-inducible factor signaling pathways in inflammatory disease. *Nitric Oxide* 25, 125–137. doi: 10.1016/j.niox.2010.12.010
- O'Neill, L. A. J., and Artyomov, M. N. (2019). Itaconate: the poster child of metabolic reprogramming in macrophage function. *Nat. Rev. Immunol.* 19, 273–281. doi: 10.1038/s41577-019-0128-5
- Papanikolaou, G., and Pantopoulos, K. (2005). Iron metabolism and toxicity. *Toxicol. Appl. Pharmacol.* 202, 199–211. doi: 10.1016/j.taap.2004.06.021
- Parisi, L., Gini, E., Baci, D., Tremolati, M., Fanuli, M., Bassani, B., et al. (2018). Macrophage polarization in chronic inflammatory diseases: killers or builders? *J. Immunol. Res.* 2018:8917804. doi: 10.1155/2018/8917804
- Peruzzotti-Jametti, L., Bernstock, J. D., Vicario, N., Costa, A. S. H., Kwok, C. K., Leonardi, T., et al. (2018). Macrophage-derived extracellular succinate licenses neural stem cells to suppress chronic neuroinflammation. *Cell Stem Cell* 22, 355–368.e13. doi: 10.1016/j.stem.2018.01.020
- Polati, R., Castagna, A., Bossi, A. M., Alberio, T., De Domenico, I., Kaplan, J., et al. (2012). Murine macrophages response to iron. *J. Proteomics* 76, 10–27.
- Puchulu-Campanella, E., Chu, H., Anstee, D. J., Galan, J. A., Tao, W. A., and Low, P. S. (2013). Identification of the components of a glycolytic enzyme metabolon on the human red blood cell membrane. *J. Biol. Chem.* 288, 848–858. doi: 10.1074/jbc.M112.428573
- Pugliese, S. C., Kumar, S., Janssen, W. J., Graham, B. B., Frid, M. G., Riddle, S. R., et al. (2017). A time- and compartment-specific activation of lung macrophages in hypoxic pulmonary hypertension. *J. Immunol.* 198, 4802–4812. doi: 10.4049/jimmunol.1601692
- Ramana, K. V., Srivastava, S., and Singhal, S. S. (2017). Lipid peroxidation products in human health and disease 2016. *Oxid. Med. Cell. Longev.* 2017:2163285.
- Rapido, F., Brittenham, G. M., Bandyopadhyay, S., La Carpia, F., L'acqua, C., McMahon, D. J., et al. (2017). Prolonged red cell storage before transfusion increases extravascular hemolysis. *J. Clin. Invest.* 127, 375–382. doi: 10.1172/JCI90837
- Rath, M., Muller, I., Kropf, P., Closs, E. I., and Munder, M. (2014). Metabolism via arginase or nitric oxide synthase: two competing arginine pathways in macrophages. *Front. Immunol.* 5:532. doi: 10.3389/fimmu.2014.00532
- Reisz, J. A., Nemkov, T., Dzieciatkowska, M., Culp-Hill, R., Stefanoni, D., Hill, R. C., et al. (2018). Methylation of protein aspartates and deamidated asparagines as a function of blood bank storage and oxidative stress in human red blood cells. *Transfusion* 58, 2978–2991. doi: 10.1111/trf.14936
- Reisz, J. A., Wither, M. J., Dzieciatkowska, M., Nemkov, T., Issaian, A., Yoshida, T., et al. (2016). Oxidative modifications of glyceraldehyde 3-phosphate dehydrogenase regulate metabolic reprogramming of stored red blood cells. *Blood* 128, e32–e42. doi: 10.1182/blood-2016-05-714816
- Remmerie, A., and Scott, C. L. (2018). Macrophages and lipid metabolism. *Cell. Immunol.* 330, 27–42. doi: 10.1016/j.cellimm.2018.01.020
- Ryan, D. G., and O'Neill, L. A. J. (2017). Krebs cycle rewired for macrophage and dendritic cell effector functions. *FEBS Lett.* 591, 2992–3006. doi: 10.1002/1873-3468.12744
- Selak, M. A., Armour, S. M., Mackenzie, E. D., Boulahbel, H., Watson, D. G., Mansfield, K. D., et al. (2005). Succinate links TCA cycle dysfunction to oncogenesis by inhibiting HIF-1alpha prolyl hydroxylase. *Cancer Cell* 7, 77–85. doi: 10.1016/j.ccr.2004.11.022
- Sica, A., and Mantovani, A. (2012). Macrophage plasticity and polarization: in vivo veritas. *J. Clin. Invest.* 122, 787–795. doi: 10.1172/JCI59643
- Soares, M. P., and Hamza, I. (2016). Macrophages and iron metabolism. *Immunity* 44, 492–504. doi: 10.1016/j.immuni.2016.02.016
- Takimoto, C. H., Chao, M. P., Gibbs, C., Mccamish, M. A., Liu, J., Chen, J. Y., et al. (2019). The Macrophage 'Do not eat me' signal, CD47, is a clinically validated cancer immunotherapy target. *Ann. Oncol.* 30, 486–489. doi: 10.1093/annonc/mdz006
- Tannahill, G. M., Curtis, A. M., Adamik, J., Palsson-Mcdermott, E. M., Mcgettrick, A. F., Goel, G., et al. (2013). Succinate is an inflammatory signal that induces IL-1beta through HIF-1alpha. *Nature* 496, 238–242. doi: 10.1038/nature11986
- Thwe, P. M., Pelgrom, L. R., Cooper, R., Beauchamp, S., Reisz, J. A., D'alessandro, A., et al. (2017). Cell-intrinsic glycogen metabolism supports early glycolytic reprogramming required for dendritic cell immune responses. *Cell Metab.* 26, 558–567.e5. doi: 10.1016/j.cmet.2017.08.012
- Van den Bossche, J., O'Neill, L. A., and Menon, D. (2017). Macrophage immunometabolism: where are we (Going)? *Trends Immunol.* 38, 395–406. doi: 10.1016/j.it.2017.03.001
- Viola, A., Munari, F., Sanchez-Rodriguez, R., Scolaro, T., and Castegna, A. (2019). The metabolic signature of macrophage responses. *Front. Immunol.* 10:1462. doi: 10.3389/fimmu.2019.01462
- Weisel, J. W., and Litvinov, R. I. (2019). Red blood cells: the forgotten player in hemostasis and thrombosis. *J. Thromb. Haemost.* 17, 271–282. doi: 10.1111/jth.14360
- Williams, N. C., and O'Neill, L. A. J. (2018). A role for the krebs cycle intermediate citrate in metabolic reprogramming in innate immunity and inflammation. *Front. Immunol.* 9:141. doi: 10.3389/fimmu.2018.00141
- Wither, M., Dzieciatkowska, M., Nemkov, T., Strop, P., D'alessandro, A., and Hansen, K. C. (2016). Hemoglobin oxidation at functional amino acid residues during routine storage of red blood cells. *Transfusion* 56, 421–426. doi: 10.1111/trf.13363
- Xu, Q., Choksi, S., Qu, J., Jang, J., Choe, M., Banfi, B., et al. (2016). NADPH oxidases are essential for macrophage differentiation. *J. Biol. Chem.* 291, 20030–20041. doi: 10.1074/jbc.M116.731216

- Yang, W. S., and Stockwell, B. R. (2016). Ferroptosis: death by lipid peroxidation. *Trends Cell Biol.* 26, 165–176. doi: 10.1016/j.tcb.2015.10.014
- Yang, Z., and Ming, X. F. (2014). Functions of arginase isoforms in macrophage inflammatory responses: impact on cardiovascular diseases and metabolic disorders. *Front. Immunol.* 5:533. doi: 10.3389/fimmu.2014.00533
- Ye, D., Guan, K. L., and Xiong, Y. (2018). Metabolism, activity, and targeting of D- and L-2-hydroxyglutarates. *Trends Cancer* 4, 151–165. doi: 10.1016/j.trecan.2017.12.005
- Yoshida, T., Prudent, M., and D'alessandro, A. (2019). Red blood cell storage lesion: causes and potential clinical consequences. *Blood Transfus.* 17, 27–52. doi: 10.2450/2019.0217-18
- Youssef, L. A., Rebbaa, A., Pampou, S., Weisberg, S. P., Stockwell, B. R., Hod, E. A., et al. (2018). Increased erythrophagocytosis induces ferroptosis in red pulp macrophages in a mouse model of transfusion. *Blood* 131, 2581–2593. doi: 10.1182/blood-2017-12-822619
- Youssef, L. A., and Spitalnik, S. L. (2017a). Iron: a double-edged sword. *Transfusion* 57, 2293–2297. doi: 10.1111/trf.14296
- Youssef, L. A., and Spitalnik, S. L. (2017b). Transfusion-related immunomodulation: a reappraisal. *Curr. Opin. Hematol.* 24, 551–557. doi: 10.1097/MOH.0000000000000376
- Yu, X. H., Zhang, D. W., Zheng, X. L., and Tang, C. K. (2019). Itaconate: an emerging determinant of inflammation in activated macrophages. *Immunol. Cell Biol.* 97, 134–141. doi: 10.1111/imcb.12218
- Zhang, J. M., and An, J. (2007). Cytokines, inflammation, and pain. *Int. Anesthesiol. Clin.* 45, 27–37.
- Zhao, R. Z., Jiang, S., Zhang, L., and Yu, Z. B. (2019). Mitochondrial electron transport chain, ROS generation and uncoupling (Review). *Int. J. Mol. Med.* 44, 3–15. doi: 10.3892/ijmm.2019.4188
- Conflict of Interest:** Although unrelated to the contents of the manuscript, the authors declare that AD'A and KCH were founders of Omix Technologies Inc. and Altis Biosciences LLC. AD'A and SS were consultants for Hemanext, Inc. SS was a consultant for Tioma, Inc., and was the Executive Director of the Worldwide Initiative for Rh Disease Eradication (WIRhE).
- The remaining authors declare that the research was conducted in the absence of any commercial or financial relationships that could be construed as a potential conflict of interest.
- Copyright © 2020 Catala, Youssef, Reisz, Dzieciatkowska, Powers, Marchetti, Karafin, Zimring, Hudson, Hansen, Spitalnik and D'Alessandro. This is an open-access article distributed under the terms of the Creative Commons Attribution License (CC BY). The use, distribution or reproduction in other forums is permitted, provided the original author(s) and the copyright owner(s) are credited and that the original publication in this journal is cited, in accordance with accepted academic practice. No use, distribution or reproduction is permitted which does not comply with these terms.